

LEVEL SET AND FAST MARCHING METHODS IN IMAGE PROCESSING AND COMPUTER VISION

R. Malladi and J.A. Sethian

Dept. of Mathematics
University of California, Berkeley 94720
http://math.berkeley.edu/~sethian/level_set.html

ABSTRACT

In recent years, level set methods have been used in a variety of settings for problems in computer vision and image processing. A related numerical methodology, known as "fast marching methods", has been recently developed to solve static Hamilton-Jacobi equations extremely quickly; the techniques rely on conversion to a static problem, and are based on a marriage between narrow band techniques for level set methods and fast sorting algorithms. We show the application of these techniques to a collection of problems, including image denoising and enhancement schemes based on curvature-controlled diffusion with automatic stopping and hierarchical scales, extremely fast shape-from-shading schemes, and shape recovery in medical imaging.

Over the past five years, level set methods have been applied to problems in image denoising and enhancement through curvature-controlled diffusion schemes. Recently, an extension of these techniques, known as fast marching methods, has been developed to solve static Hamilton-Jacobi equations which arise in aspects of computer vision. In this paper, we discuss recent advances in both of these techniques for such problems.

1. LEVEL SET METHODS

Level set techniques, [7, 8, 10] numerically approximate the equations of motion for a propagating front by transforming them into an initial value partial differential equation whose unique solution gives the position of the front. They were introduced by Osher and Sethian in [7], and rely on a fundamental entropy condition for propagating fronts introduced in Sethian [9]. In this setting, corners and cusps are naturally handled, and topological change occurs in a straightforward and rigorous manner. Complex motion, particularly those that require surface diffusion, sensitive dependence on normal directions to the interface, and sophisticated breaking and merging, result from a straightforward implementation of the scheme, with no user intervention.

More precisely, level set methods view a moving interface as the zero level set of a function $\phi(x, t = 0)$. An

This work was supported in part by the Applied Mathematical Science subprogram of the Office of Energy Research, U.S. Department of Energy, under Contract Number DE-AC03-76SF00098, and the Office of Naval Research under grant FDN00014-96-1-0381.

evolution equation for the interface moving with speed F in its normal direction is given [7] by

$$\phi_t + F|\nabla\phi| = 0, \quad (1)$$

The surface $\phi = 0$ corresponding to the propagating hypersurface may change topology, as well as form sharp corners, Finite differences lead to a numerical scheme to approximate the solution, and intrinsic geometric properties (normal vectors and curvature) are easily determined from the level set function.

The key in level set methods is to approximate the gradient in the level set equation in a way that satisfies the correct entropy condition. One of the simplest such schemes is given in [7], namely

$$\begin{aligned} \phi_{ij}^{n+1} = & \phi_{ij}^n - \Delta t F_{ij} (\max(D_{ij}^{-x}\phi, 0)^2 + \min(D_{ij}^{+x}\phi, 0)^2) \quad (2) \\ & + \max(D_{ij}^{-y}\phi, 0)^2 + \min(D_{ij}^{+y}\phi, 0)^2)^{1/2}, \quad (3) \end{aligned}$$

The crucial point in this (any such appropriate) numerical scheme is the correct direction of the unwinding and treatment of sonic points. Here, we have assumed that the speed function F is essentially an advection term. In the case where F contains a curvature component (such as $F = -\kappa$), the curvature term is approximated through a central difference approximation. The formulation is unchanged for propagating interfaces in three dimensions.

Since their introduction, level set techniques have been used in a wide collection of problems involving moving interfaces, including the generation of minimal surfaces, singularities and geodesics in moving curves and surfaces, flame propagation, etching, deposition and lithography calculations, crystal growth, and grid generation; see [10] for an extensive review.

2. FAST MARCHING METHODS

Fast marching methods were introduced by Sethian [11, 8] for a special case of front evolution. Consider the case of a front moving with speed $F = F(x, y)$ where F is always either positive or negative. Then let $T(x, y)$ be the time at which the curve crosses the point (x, y) . The surface $T(x, y)$ then satisfies the equation

$$|\nabla T|F = 1. \quad (4)$$

On the basis of the above discussion, we know that we must use an upwind, entropy-satisfying scheme to the gradient to approximate the gradient. Using the above scheme, we have

$$\left[\begin{array}{l} \max(D_{ij}^{-x}T, 0)^2 + \min(D_{ij}^{+x}T, 0)^2 \\ + \max(D_{ij}^{-y}T, 0)^2 + \min(D_{ij}^{+y}T, 0)^2 \end{array} \right]^{1/2} F_{ij} = 1., \quad (5)$$

The fast marching method systematically advances the front in an upwind fashion to produce the solution T . The key is the observation that the upwind difference structure of Equation (5) means that information propagates “one way”, that is, from smaller values of u to larger values. Hence, the fast marching algorithm rests on “solving” Equation (5) by building the solution outwards from the smallest u value. The algorithm is made fast by confining the “building zone” to a narrow band around the front, motivated by the narrow band technology introduced in Chopp [10], used in recovering shapes from images in Malladi, Sethian and Vemuri [6], and analyzed extensively by Adalsteinsson and Sethian in [10]. The idea is to sweep the front ahead in an upwind fashion by considering a set of points in narrow band around the existing front, and to march this narrow band forward, freezing the values of existing points and bringing new ones into the narrow band structure. The key is in the selection of *which* grid point in the narrow band to update.

The algorithm is as follows: First, we points in the initial conditions as “Alive”. We then tag as “Close” all points one grid down. Finally, we tag as “Far” all other grid points. Then the loop is

1. Begin Loop: Let $Trial$ be the point in “Close” with the smallest value for T .
2. Add the point $Trial$ to $Alive$; remove it from “Close”
3. Tag as “Close” all neighbors of $Trial$ that are not “Alive” If the neighbor is in “Far” remove it from that list and add it to the set $Close$.
4. Recompute the values of T at all neighbors according to Eqn. 5, selecting the largest possible solution to the quadratic equation.
5. Return to top of Loop:

This algorithm works because the process of recomputing the T values at upwind neighboring points cannot yield a value smaller than any of that at any of the accepted points. Thus, we can march the solution outwards, always selecting the narrow band grid point with minimum trial value for u , and readjusting neighbors. Another way to look at this is that each minimum trial value begins an application of Huygen’s principle, and the expanding wave front touches and updates all others. The speed of the algorithm comes from a heapsort technique to efficiently locate the smallest element in the set $Trial$. For details, see [8, 11, 10].

The technique also can be extended to more general static Hamiltonians of the form

$$H(Du, x) = 0 \quad (6)$$

where Du is represents the derivatives in each of the component variables u_{x_1}, \dots, u_{x_N} . In all cases, the scheme is extremely fast; if there are N total points in the grid, then the scheme solves the equation in $O(N \log N)$.

3. MIN/MAX FLOW FOR IMAGE DENOISING AND ENHANCEMENT: LEVEL SET METHODS

Define an *image* to be an intensity map $I(x, y)$ given at each point of a two-dimensional domain. The range of the function $I(x, y)$ depends on the type of image; for black and white image the range is either 0 or 255, for grey-scale images $I(x, y)$ is a function mapped between 0 and 255. In their seminal work, Alvarez, Lions and Morel ([1]) introduced a noise removal scheme by employing, in part, some ideas about curvature flow and level set equations. Their basic idea was to flow iso-intensity contours under curvature flow; An attractive quality of this motion is that sharp boundaries are preserved; smoothing takes place inside a region, but not across region boundaries. This work opened up a wide collection of partial differential equations-based schemes for image processing; see [1].

In Malladi and Sethian [4], a curvature-based flow algorithm was developed which exploits a “min/max” function to select the type of curvature motion desired to remove noise. This approach has two desirable features:

1. There is an intrinsic, adjustable definition of scale within the algorithm, such that all noise below that level is removed, and all features above that level are preserved.
2. The algorithm stops automatically once the sub-scale noise is removed; continued application of the scheme produces no change.

To understand this scheme, consider the equation

$$\phi_t = \bar{F}|\nabla\phi|. \quad (7)$$

Grayson showed [2] that a curve collapsing under its curvature will correspond to speed $\bar{F} = \kappa$. Now, consider two variations on the basic curvature flow, namely

- $\bar{F}(\kappa) = \min(\kappa, 0.0)$
- $\bar{F}(\kappa) = \max(\kappa, 0.0)$

Here, we have chosen the negative of the signed distance in the interior, and the positive sign in the exterior region. The effect of flow under $\bar{F}(\kappa) = \min(\kappa, 0.0)$ is allow the inward concave fingers to grow outwards, while suppressing the motion of the outward convex regions. Thus, the motion halts as soon as the convex hull is obtained. Conversely, the effect of flow under $\bar{F}(\kappa) = \max(\kappa, 0.0)$ is to allow the outward regions to grow inwards while suppressing the motion of the outward convex regions. Thus, the motion halts as soon as the convex hull is obtained. Conversely, the effect of flow under $\bar{F}(\kappa) = \max(\kappa, 0.0)$ is to allow the outward regions to grow inwards while suppressing the motion of the inward concave regions. However, once the shape becomes fully convex, the curvature is always positive and the flow becomes the same as regular curvature flow.

Our goal is to select the correct choice of flow that smoothes out small oscillations, but maintains the essential properties of the shape. In order to do so, we discuss the idea of the min/max switch.

Consider the following speed function, introduced in [4]:

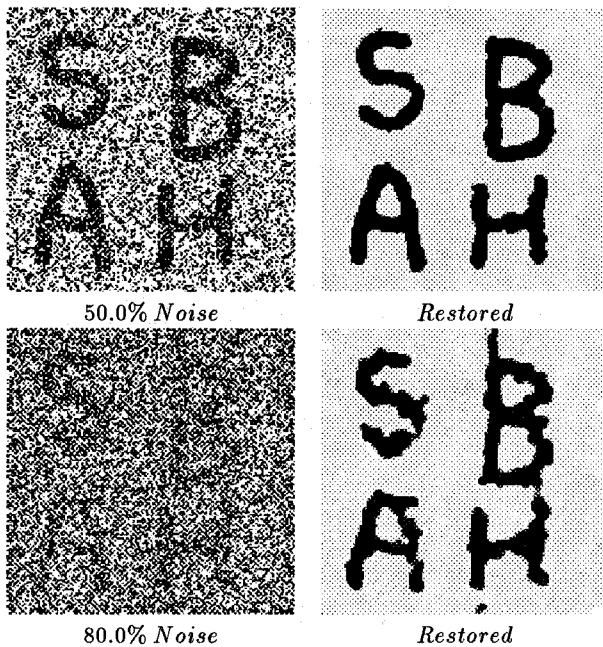


Figure 1: Image restoration of Binary Images with Grey-Scale Salt-and-Pepper Noise Using Min/Max Flow: Restored shapes are final shape obtained ($T = \infty$).

$$\bar{F}_{\min/\max}^{Stencil=k} = \begin{cases} \min(\kappa, 0) & \text{if } Ave_{\phi(x,y)}^{R=kh} < 0 \\ \max(\kappa, 0) & \text{if } Ave_{\phi(x,y)}^{R=kh} \geq 0 \end{cases} \quad (8)$$

where $Ave_{\phi(x,y)}^{R=kh}$ is defined as the average value of ϕ in a disk of radius $R = kh$ centered around the point (x, y) . Here, h is the step size of the grid. Thus, given a “StencilRadius” k , the above yields a speed function which depends on the value of ϕ at the point (x, y) , the average value of ϕ in neighborhood of a given size, and the value of the curvature of the level curve going through (x, y) .

In Figure 1, 50% and 80% grey-scale noise is added to a black and white image of a hand-written character. The noise is added as follows: $X\%$ noise means that at $X\%$ of the pixels, the given value is replaced with a number chosen with uniform distribution between 0 and 255. Here, the min/max switch function is taken relative to the value 127.5 rather than zero. The restored figures are converged. Continued application of the scheme yields almost no change in the results. We refer the reader to [4] for further applications of this scheme in enhancement of grey-scale and color images, edge finding, and its link to accurate shape recovery. The techniques can be extended to gray-scale images, as well as three-dimensional images; for details, see [5].

4. SHAPE-FROM-SHADING: FAST MARCHING METHODS

The fast marching method provides an extremely fast way of solving the so-called shape-from-shading problem (see

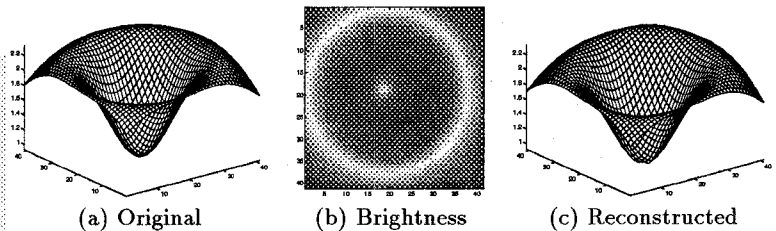


Figure 2: Shape-from-shading reconstruction of Double Gaussian surface

[10] and the references therein). Suppose we illuminate a non-self-shadowing surface $T(x, y)$ from a single point light source. Let (α, β, γ) be the direction from the light source. In the simplest case of a Lambertian surface, the brightness map $I(x, y)$ is given in a very simple form by

$$I(x, y) = (\alpha, \beta, \gamma) \cdot n. \quad (9)$$

Thus, the shape-from-shading problem is to reconstruct the surface $T(x, y)$ given the brightness map $I(x, y)$.

Consider the simplest case, namely that in which the light comes from straight down. Then the light source vector is $(0, 0, 1)$, and we then have an Eikonal equation for the surface, namely

$$|\nabla T| = \sqrt{\frac{1}{T^2} - 1}. \quad (10)$$

As an example, taken from [10], we use a double Gaussian function of the form

$$T(x, y) = 3e^{-(x^2+y^2)} - 2e^{-20((x-.05)^2+(y-.05)^2)} \quad (11)$$

We compute the brightness map and then reconstruct the surface, see Figure 2; again, the result is computed in $O(N \log N)$.

5. SHAPE RECOVERY: LEVEL SET AND FAST MARCHING METHODS

Imagine that one is given an image. The goal in *shape detection/recovery* is to extract a particular shape from that image; here, “extract” means to produce a mathematical description of the shape which can be used in a variety of forms. Our approach (see [6]) is motivated by the active force contour/snake approach to shape recovery. We start an initial front inside the desired region, and let it propagate outwards with a speed function that stops the motion when the boundary is reached. Here, we provide some background for this technique, and then described a hybrid level set/fast marching technique to quickly extract the desired shape.

More precisely, consider a speed function of the form $1 - \epsilon\kappa(-1 - \epsilon\kappa)$, where ϵ is a constant. As discussed earlier, the constant acts as an advection term, and is independent of the moving front’s geometry. The front uniformly expands (contracts) with speed 1 (-1) depending on the sign, and is analogous to an inflation force. The diffusive second term $\epsilon\kappa$ depends on the geometry of the front and smooths out the high curvature regions of the front.

Our goal now is to define a speed function from the image data that acts as a halting criterion for this speed function. The front moves under a simple speed law $F = 1 - \epsilon\kappa$ by solving an initial value partial differential equation on the function ψ . The driving force for this comes from applying artificial image-based speed terms on the surface. The first term causes the surface to stop in the vicinity of desired shape boundaries; the second term stabilizes the front around the same boundaries. Specifically, the equation of motion is

$$\psi_t + k_I(1 - \epsilon\kappa)|\nabla\psi| - \beta\nabla P \cdot \nabla\psi = 0. \quad (12)$$

Here, the term

$$k_I = \frac{1}{1 + |\nabla G_\sigma * I(x, y, z)|} \quad (13)$$

causes the surface to have speeds very close to 0 near high image gradients, i.e., possible edges. False gradients due to noise can be avoided by applying a Gaussian smoothing filter or the previously discussed edge-preserving smoothing scheme. The second term $\nabla P \cdot \nabla\psi$ denotes the projection of an (attractive force) vector normal to the surface. This force which is realized as the gradient of a potential field

$$P(x, y, z) = -|\nabla G_\sigma * I(x, y, z)|, \quad (14)$$

attracts the surface to the edges in the image; the coefficient β controls the strength of this attraction.

The above front propagation equation was solved using a level set technique in [6]. However, in the absence of curvature and the last term, the equation becomes a static Hamilton-Jacobi equation, and can be solved using the fast marching method. This suggests the hybrid technique introduced in [3]; namely that first, the fast marching method, together with an stopping criterion synthesized from the image, is used to quickly find a close approximation to the shape, followed by application of the narrow band level set method to execute the final stages of shape extraction. In Figure 3, this hybrid technique is applied to the extraction of a three-dimensional scan of the brain and of the heart.

6. REFERENCES

- [1] Alvarez, L., Lions, P.L., and Morel, M., *Image Selective Smoothing and Edge Detection by Nonlinear Diffusion. II*, SIAM J. Num. Anal. 29, 3, 845–866, 1992.
- [2] Grayson, M., *The Heat Equation Shrinks Embedded Plane Curves to Round Points*, J. Diff. Geom., 26, pp. 285, 1987.
- [3] Malladi, R., and Sethian, J.A., *An $O(N \log N)$ Algorithm for Shape Modeling*, accepted, to appear, Proc. Nat. Acad. Sci., 1996.
- [4] Malladi, R., and Sethian, J.A., *Image Processing via Level Set Curvature Flow*, Proc. Natl. Acad. of Sci., 92, 15, pp. 7046–7050, 1995.
- [5] Malladi, R., and Sethian, J.A., *Level Set Methods for Curvature Flow, Image Enhancement, and Shape Recovery in Medical Images*, to appear, Proc. of Conf. on Visualization and Mathematics, June, 1995, Berlin, Germany, Springer-Verlag, in press.
- [6] Malladi, R., Sethian, J.A., and Vemuri, B.C., *Shape Modeling with Front Propagation: A Level Set Approach*, IEEE Trans. on Pattern Analysis and Machine Intelligence, 17, 2, pp. 158–175, 1995.
- [7] Osher, S., and Sethian, J.A., *Fronts Propagating with Curvature Dependent speed: Algorithms Based on Hamilton-Jacobi Formulation*, J. Comp. Phys., Vol. 79, pp. 12–49, 1988.
- [8] Sethian, J.A., *A Review of the Theory, Algorithms, and Applications of Level Set Methods for Propagating Interfaces*, Acta Numerica, 1996.
- [9] Sethian, J.A., *Curvature and the Evolution of Fronts*, Comm. Math. Phys., Vol. 101, pp. 487–499, 1985.
- [10] Sethian, J.A., *Level Set Methods: Evolving Interfaces in Geometry, Fluid Mechanics, Computer Vision and Material Science*, Cambridge University Press, 1996.
- [11] Sethian, J.A., *A Marching Level Set Method for Monotonically Advancing Fronts*, Proc. Nat. Acad. Sci., 93, 4, pp.1591–1595, 1996.

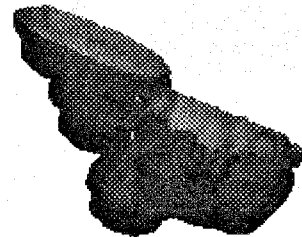
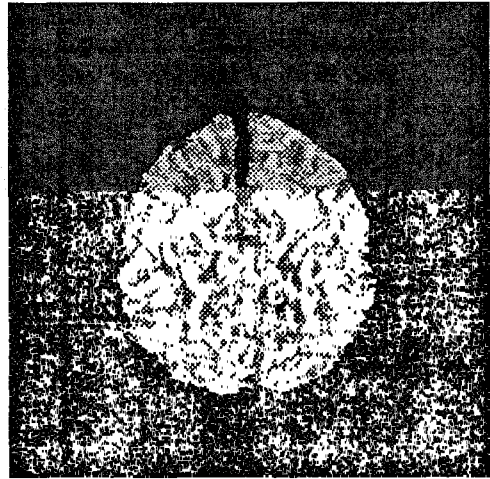


Figure 3: Shape Recovery of Three-Dimensional Brain and Heart Chambers from MRI